Journal of Magnetic Resonance 305 (2019) 180–184

Contents lists available at ScienceDirect

Journal of Magnetic Resonance

journal homepage: www.elsevier.com/locate/jmr

RF shielding and eddy currents in NMR probes

Mark S. Conradi [a,*], Albert P. Zens [b]

[a] ABQMR, Inc., 2301 Yale Blvd SE, Suite C2, Albuquerque, NM 87106, USA
[b] JEOL, 10 Dearborn Road, Peabody, MA 01960, USA

ARTICLE INFO

Article history:
Received 4 May 2019
Revised 17 June 2019
Accepted 21 June 2019
Available online 3 July 2019

Keywords:
Shielding
Skin depth
NMR probes
Eddy currents
rf heating
Infrared shielding
Gradients

ABSTRACT

Shielding of the NMR sample by a thin coating of metal between the sample and the rf coil arises in some geometries. The shielding may be used for rf heating of the sample tube or for a high infrared reflectivity coating in cryoprobe applications. An important application is for a shield that prevents noise from entering the rf probe circuit while allowing pulsed magnetic field gradients or field modulation to pass. We show by simple, approximate derivations that the criterion for shielding is not whether the coating exceeds the classical electromagnetic skin depth δ at the operating frequency (as is often stated), but whether the geometric mean between the thickness and an appropriate radius r exceeds δ. Thus, because r is typically much larger than δ, conducting layers substantially thinner than δ may still be good shields. Measurements are performed at high audio frequencies to confirm the calculations, using geometries relevant to rf saddle coils and to rf solenoids. Measurements of the slowing of the edges of a pulsed field gradient are also in accord with the calculations.

1. Introduction

There are uses in NMR probes for shielding between the sample and the rf coil. These include resistive layers to allow off-resonance rf heating [1] of the glass sample tube and the sample within and low infrared-emissivity layers in cryoprobes [2]. Of course, the aim is that most of the coil's rf field passes through to the sample. A related and important application is a rf shield that is virtually transparent to the low frequency fields of a pulsed magnetic field gradient [3]. Another use is the sidewalls of an ESR cavity that must be good shields at the microwave frequency and yet pass the field modulation (typically at 100 kHz) with little attenuation [4–6]. In ENDOR work, the rf NMR coil may reside outside the plastic microwave cavity [7]; the rf field may need to penetrate thin microwave shielding.

Many workers believe that whether the layer shields or passes the ac field depends solely on whether the shield thickness is greater or less than the electromagnetic skin depth δ [8–10]. But we show here that this is not the correct criterion. We present simple, approximate calculations that show the relevant quantity (for comparison to δ) is the geometric mean of the thickness and an appropriate radius of the eddy current paths. Measurements presented here confirm this.

We remark that our derivations are not new electromagnetism [8–11]. Instead, the calculations are aimed at delivering intuitive understanding and correcting widely held misconceptions. The engineering literature discusses related treatments, for general shielding applications and for use of SQUID detectors of weak magnetic fields [12–15].

2. Calculations

We consider a circular planar loop of conductor (the shield), with outer radius r_o and inner radius r_i; the thickness is t, with t much smaller than the radii (see Fig. 1a). The loop sits in a uniform ac magnetic field B_1 at frequency ω, normal to the plane of the loop. We will say no further details about the source of B_1, except that it is evidently the transmitter coil and is assumed to be much larger than the shield for calculational ease. We are interested in the extent to which the field at the center of the loop is shielded by the eddy current I induced in the loop. The magnetic flux ϕ [10] through the loop (flux is field times area) is the sum of the externally generated flux B_1A (where A is the area of the loop, πr^2, with r the average of the inner and outer radii) and the flux LI from the eddy current I, with L the self-inductance of the loop;

$$\Phi = B_1A + LI. \quad (1)$$

* Corresponding author.
E-mail address: msc@wuphys.wustl.edu (M.S. Conradi).

https://doi.org/10.1016/j.jmr.2019.06.011
1090-7807/

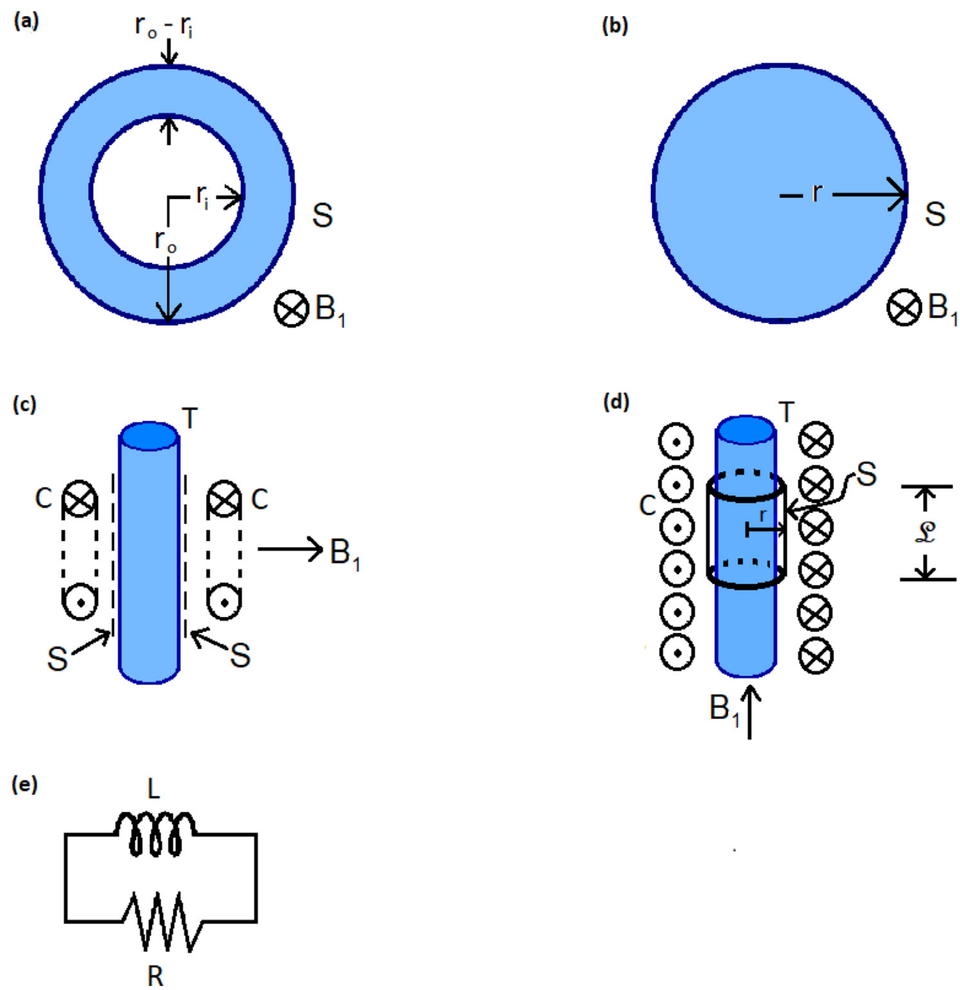

Fig. 1. Geometries of shields. C is the rf coil and S is the shield; T is the NMR tube. B_1 is the nominal field direction. (a) Planar annular disk of thickness t is morphed into (b) full planar disk. A saddle or Helmholtz pair C in (c) surrounds a tube T and shields S. A solenoidal coil in (d) has magnetic field parallel to the cylindrical shield axis; $\mathscr{L}$ is the length of the shield. (e) Equivalent LR circuit of shield.

The eddy current I is just the induced EMF or voltage ($-d\phi/dt$, Faraday's induction) divided by the resistance R of the loop. Using the resistivity ρ and recalling resistance R is ρ times path length divided by path cross-sectional area,

$$R = \rho 2\pi r/(r_0 - r_i)t. \tag{2}$$

Thus, the current I is given by

$$I = -i\omega(B_1 A + LI)/R. \tag{3}$$

Here we take all ac quantities to oscillate exp(iωt) so that time derivatives are given by multiplying by iω. The current I in (3) is found algebraically,

$$I(1 + i\omega L/R) = -i\omega B_1 A/R \tag{4}$$

So the total field B_{tot} inside the coil, just ϕ/A, becomes from (1) and (4),

$$B_{tot} = B_1 + LI/A = B_1\left\{1 - \left[\frac{\frac{i\omega L}{R}}{1 + \frac{i\omega L}{R}}\right]\right\}. \tag{5}$$

The ratio B_{tot}/B_1 becomes,

$$B_{tot}/B_1 = 1 - [i\omega\tau/(1 + i\omega\tau)] = 1/(1 + i\omega\tau), \tag{6}$$

where ωτ = ωL/R is dimensionless, with τ being the time constant of eddy currents, τ = L/R (as in circuit of Fig. 1e).

The result is simple, with the fraction of the original field now at the center given by 1/(1 + iωτ). Evidently the field at the center is not only attenuated, but phase-shifted as well. This is the same expression for the response of a simple low-pass RC filter, with time constant τ = RC; the shielding loop here is a low-pass filter. When $\omega\tau \gg 1$, the shielding is good, with $B_{tot} \ll$ the original field B_1. But for $\omega\tau \ll 1$, the field at the center is nearly equal to the original, unshielded field.

Now we approximate the inductance L of our loop [10]. By definition, L = ϕ/I; the self-field B at the center of the loop is $\mu_0 I/2r$, so the inductance is

$$L = \pi r^2 \mu_0/2r = \mu_0 \pi r/2. \tag{7}$$

This takes the self-field B as uniform within the plane of the loop, which it is not. Thus, this is only an approximation. So, using Eq. (2) for the resistance R, the time constant τ (see LR circuit of Fig. 1e) becomes

$$\tau = L/R = (\mu_0 \pi r/2)(r_0 - r_i)t/\rho 2\pi r = \mu_0(r_0 - r_i)t/4\rho. \tag{8}$$

We now use the annular loop in Fig. 1a to represent the solid sheet with vanishing r_i, as in Fig. 1b. Thus, in Eq. (8) we use r as the average radius of the eddy current paths and r_o-r_i is approximated as r. With these approximations, the time constant τ = L/R for the solid sheet of Fig. 1b is just

$$\tau = \frac{\mu_0 r t}{4\rho}. \tag{9}$$

And the crucial shielding parameter ωτ is

$$\omega\tau = rt/(4\rho/\mu_0\omega) = rt/2\delta^2, \tag{10}$$

where we recognized the classical electromagnetic skin depth δ,

$$\delta = \sqrt{2\rho/\mu_0\omega}. \tag{11}$$

The factor of 2 in Eq. (10) is unreliable, given the approximations made. The formula for δ is in MKS-SI units and applies for the high conductivity limit, as appropriate for metals [10].

In Eq. (10), in terms of the geometric mean √(rt), √(rt) ≫ δ means ωτ ≫ 1 and good shielding (see Eq. (6)), while √(rt) ≪ δ means ωτ ≪ 1 and poor shielding. We note that since the eddy current radius r is almost always large compared to the skin depth δ, some thicknesses t that are small compared to δ may yet satisfy √(rt) ≫ δ and be very effective shields. Specifically, good shielding requires that t ≫ δ^2/r = δ/(r/δ). That is, the thickness t needs only to be greater than a small fraction of δ; the fraction is $(r/\delta)^{-1}$. This is the core result presented here.

The geometry of Fig. 1a and b is directly relevant to the saddle or Helmholtz pair rf coil, where its rf field tries to penetrate or thread the rf shield (wrapped around a tube) transverse to the tube axis, as in Fig. 1c. We see little distinction between one or two planar rf shields and a shield that is curved around the tube.

Next, we consider the geometry shown in Fig. 1d using a field B_1 generated by a solenoid, with B_1 along the axis of the cylindrical shield. Here the eddy current I flows along the shield, around the axis. For a shield of length $\mathscr{L}$, thickness t, and radius r, the resistance R is,

$$R = \rho 2\pi r/(\mathscr{L}t). \tag{12}$$

The inductance L is given by ϕ/I as usual, with the shield acting as a 1-turn long solenoid (here we assume $\mathscr{L}$ ≫ r) with self-field B = μ_0I/$\mathscr{L}$ in the long solenoid approximation [10],

$$L = \pi r^2\mu_0/\mathscr{L}. \tag{13}$$

The time constant τ is L/R so the crucial parameter for shielding ωτ is,

$$\omega\tau = rt/(2\rho/\mu_0\omega) = rt/\delta^2 = [\sqrt{rt}/\delta]^2. \tag{14}$$

As in the flat geometry, the issue of shielding reduces to whether the geometric mean of t and r is less than or greater than the classical skin depth, δ. Here the radius of the eddy current path is clearly the radius r of the cylinder.

The two geometries, planar and cylindrical, may appear quite different at first. However, in both cases the rf field B_1 is trying to thread through or penetrate a conducting loop of radius r and thickness t. The cylindrical shield could be distorted into a planar shield if the shield were elastic. So, it is not surprising that their criteria for good shielding are essentially the same.

The fundamental difference between the present results and that of the classical skin depth [8,10] is that the geometries are very different. Here the field tries to penetrate a closed conducting path, with the field *normal* to the conducting path. In the skin depth calculation, an E-M plane wave with fields E and B *transverse* (in the plane of the conductor) tries to propagate through the conductor. The skin depth also describes the depth of the current flow. So, our calculation describes rf field trying to thread a conducting loop and the skin depth calculation describes rf magnetic field trying to traverse the conducting material itself.

3. Experiments

To test this matter at radio frequencies, the required foil thicknesses can be very thin, necessitating vapor deposition methods. To avoid these methods and the uncertainties of the deposited layer thickness, we used commercially available foils and thin-wall tubes, driving the experiments down into the high audio frequency range. Of course, the same principles apply for all thicknesses and frequencies; our choice is a matter of experimental convenience.

Measurements were performed from 2 kHz to 150 kHz using a flat "transmitting" coil of radius 0.8 in. (2 cm) and 50 turns and a similar pickup (detection) coil, separated by one inch (2.54 cm) along their common axis. An audio generator drove a Kenwood high-fidelity power amplifier to excite the transmitting coil. An oscilloscope was used to measure the pickup coil voltage. The transmission ratio $|\mathscr{R}|$ of the detected voltage with/without a conducting foil shield interposed between the two coils is reported in Fig. 2 as filled symbols. In detail the conducting foil was 10 cm × 15 cm, much larger than the coils, to make it difficult for magnetic flux to "go around" the shield. The entire assembly was built into an aluminum box to provide shielding from external interference fields. As presented in Fig. 2, the ratio $|\mathscr{R}|$ is nearly unity at low frequencies and drops to nearly zero at high frequencies, typical of a low-pass filter. In Table 1, we report the frequency F such that the transmission ratio $|\mathscr{R}| = |1/(1+i)| = 0.71$. This numerical choice of the "cut-off" frequency corresponds to ωτ = 1 in Eqs. (6) and (14), so √(rt) = δ. We note that our approximate derivations are unreliable to factors of order 2, as mentioned earlier.

In Table 1, we compare the geometric mean of the radius r and the thickness t (that is, √(rt)) to the skin depth δ at cut-off frequency F. This is performed for three cases: (a) an aluminum foil of 0.001 in. thickness (0.0254 mm), (b) a shield made of 4 layers of the same aluminum foil with insulation paper in between the layers (the currents try to flow within each foil so the insulation is of no importance), and (c) a single brass foil of thickness 0.005 in. (0.127 mm). The tabulated resistivities of aluminum and brass are 2.65 microohm-cm and 7 microohm-cm, respectively; these values and the experimental values of F are used to calculate δ from Eq. (11) in each case. For the average radius r of the eddy currents, we use the radius of the driving coil. The results show that √(rt) is close to δ at frequency F while the thickness t is much smaller than δ. This confirms the prediction of the calculations. The deviation of √(rt)/δ from unity as in Table 1 is a result of the broad approximations made in the calculation.

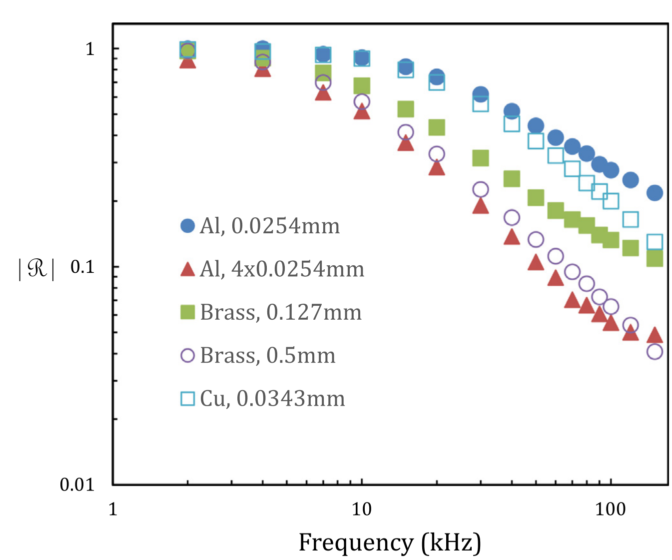

Fig. 2. Transmission ratio $|\mathscr{R}|$ of flat foil shields (filled symbols) and thin-wall cylinders (open symbols), as a function of frequency (in kHz). The behavior is that of a lowpass filter. Note the logarithmic scales.

Table 1
Results from measured transmission ratios through shields.

Material, resistivity ρ (μΩ cm)	Al, 2.65	Al, 2.65	Brass, 7.0	Brass, 7.0	Cu, 1.68
Shape	Flat	Flat	Flat	Tube	Tube
Thickness (mm)	0.0254	4 × 0.0254	0.127	0.5	0.0343
Radius r (mm)	20	20	20	6.35	8.1
Cut-off freq F (kHz)	24	6.35	9.8	7.2	20.2
Skin depth δ at F (mm)	0.53	1.03	1.35	1.57	0.45
$\sqrt{rt}/\delta$	1.34	1.38	1.18	1.13	1.18
t/δ	0.048	0.10	0.095	0.32	0.076

We also used a geometry suitable for rf solenoids, as in Fig. 1d. Here a large coil (flat, 50 turns, as used earlier) is driven by the audio power amplifier and a small pick-up coil sits in the middle of the driven coil. The pick-up is approximately 200 turns on an 8 mm diameter wooden dowel rod. A shield of metal tubing 4 cm long can be installed or removed and the pick-up voltage amplitudes compared, to form ratio $|\mathcal{R}|$. Two cases were used, one with a 0.5 in. (12.7 mm) diameter brass tube of thickness 0.020 in. (0.5) mm, and a copper foil formed into a cylinder of diameter 0.64 in. (16.2 mm) and thickness 0.00135 in. (0.034 mm). This tube was seamed with soft solder, with attention paid to minimize the thickness of the solder to avoid additional resistance from the solder.

The results for ratio $|\mathcal{R}|$ as a function of frequency are presented as open symbols in Fig. 2. We note that all the data, from tubes as well as flat foils, appear to obey nearly the same functional dependence but with different cut-off frequencies; they appear horizontally shifted along the logarithmic frequency axis. Again, the cut-off frequencies F were found for each case where the ratio $|\mathcal{R}|$ is 0.71, corresponding to $\omega\tau = 1$. Table 1 lists the cut-off frequencies F as well as thickness t and the skin depth δ calculated at F. Here we see good agreement between $\sqrt{(rt)}$ and δ, with $\sqrt{(rt)}/\delta$ values near unity. The values of t/δ are much smaller than one. Thus, shields less thick than δ can yet be good shields.

Gradient coil shielding: An important application of the shielding issue is the shielding of gradient fields used in MRI. In an application in our lab, we have a 35.6 cm diameter 3-axis gradient coil as part of a large 2 MHz MRI scanner. It is shielded from the smaller rf coil by a rf copper shield of 29 cm diameter. We wondered how badly the shield slowed down the rising and falling edges of the gradient waveform. Because most gradients are specified in the time domain, we chose to work in time domain, rather than the frequency domain used in the measurements described above.

The copper shield was 29 cm diameter and 63 cm long, with thickness of 0.0343 mm. A pick-up coil of 12.5 cm diameter was located centrally, axially and radially, within the shield. Half of its 30 turns were wound clockwise and the other half counterclockwise, in series. The two halves were spaced by 25 cm so that it was truly a longitudinal *gradient* pick-up coil. The pick-up coil voltage was RC integrated to yield the actual gradient waveform G (the coil itself generates dG/dt by Faraday induction). The large sending gradient coil (generating longitudinal or axial gradient) was driven with a 1–2 kHz square wave (so, showing both rising and falling edges). The square wave was amplified by the Kenwood audio amplifier. With 350 Ω placed in series with the (low impedance) amplifier output, this is a controlled-current source, as used routinely in MRI. The current and gradient waveforms are thus crisp square waves.

With no shield, the picked-up gradient waveform has rise and fall times of about 3 μs. This is due to the finite bandpass of the system. With the shield in place between the gradient coil and the pick-up coil, the risetime increased to 100 (±20) μs. Clearly the initial 3 μs is negligible here and all the 100 μs belongs to the shield. Using Eq. (14), the time constant τ is computed to be 197 μs. The computed value from Eq. (14) is correct only for a uniform field. But for the gradient field, there are important transverse field components that penetrate the shield, too; thus the 197 μs value must be taken as only approximate.

The cut-off frequencies (1/τ) of the shielding low-pass filter effect are 10,000 and 5000 s^{-1}, from the experimental and calculated values of τ, respectively. The value of ω for which the shield is one skin depth thick from Eq. (11) is much, much larger at 22×10^6 s^{-1}. Clearly, if one thought that only the skin depth mattered here, the observed slowing of the gradient waveform would be a surprise. The large ratio between the cut-off frequencies computed these two ways is due to the large ratio of r/t here (about 4400).

We note that the shield thickness is about one skin depth at our 2 MHz MRI frequency. Thus, to increase the Q of the rf coil, we would benefit from using a thicker shield, decreasing the rf losses due to currents in the shield. Of course, it would slow down the edges of the gradient fields even more.

4. Conclusions

The question of whether a foil or a cylinder does a good job of shielding an ac field at ω is not simply an issue of whether the conductor thickness t exceeds the classical electromagnetic skin depth δ. Instead, the issue is whether the dimensionless parameter ωτ exceeds unity, with τ being the shield's inductive time constant L/R. In turn, the parameter ωτ is given approximately by rt/δ^2. Thus, shielding depends on the geometric mean of t with the average radius r of eddy currents divided by the skin depth δ. Because the radius r is generally much larger than δ, a conductor with thickness smaller than the classical skin depth δ may still be a good shield. Likewise, gradient waveform components (or field modulation) at frequency F can be filtered (and the waveform "slowed"), even by rf shielding layers thinner than the skin depth at F.

The results have implications for rf heating by conducting layers on the glass NMR tube, passing modulation fields through end plates of ESR cavities, making rf shielding transparent to pulsed field gradients, and low-emissivity coatings used in cryoprobes.

Acknowledgment

The authors appreciate the suggestions of references by an anonymous reviewer.

References

[1] G.G. Maresch, R.D. Kendrick, C.S. Yannoni, High-temperature nmr using inductive heating, Rev. Sci. Instrum. 61 (1990) 77–80.
[2] A.P. Zens, private communication.
[3] H. Han, M. Ouellette, B. MacMillan, F. Goora, R. MacGregor, D. Green, B.J. Balcom, High pressure magnetic resonance imaging with metallic vessels, J. Magn. Reson. 213 (2011) 90–97.
[4] C.P. Poole, Electron Spin Resonance, Interscience, New York, 1967.
[5] G. Casini, P. Graziani, R. Linari, A. Tronconi, X-band cavity for low-temperature electron spin resonance experiments, Rev. Sci. Instrum. 47 (1976) 318–320.
[6] K.M. Evenson, D.S. Burch, X band esr cavity for studies of paramagnetic gases, Rev. Sci. Instrum. 37 (1966) 236–237.
[7] H.L. Van Camp, C.P. Scholes, R.A. Isaacson, Plastic endor cavity for studies of biological compounds at 2 K, Rev. Sci. Instrum. 47 (1976) 516–517.

[8] J.D. Jackson, Classical Electrodynamics, John Wiley, New York, 1962.
[9] E.M. Purcell, Electricity and Magnetism, McGraw Hill, New York, 1965.
[10] D.J. Griffiths, Introduction to Electrodynamics, third ed., Prentice Hall, Upper Saddle River NJ, 1999.
[11] R.L. Stoll, The Analysis of Eddy Currents, Clarendon Press, Oxford UK, 1974.
[12] J.E. Bridges, An update on the circuit approach to calculate shielding effectiveness, IEEE Trans. Electromagn. Compatib. 30 (1988) 211–221.
[13] P. Heinonen, M. Tuomola, J. Lekkala, J. Malmivuo, Properties of a thick-walled conducting enclosure in low-frequency magnetic shielding, J. Phys. E: Sci. Instrum. 13 (1980) 569–570.
[14] J.E. Zimmerman, "SQUID instruments and shielding for low-level magnetic measurements, J. Appl. Phys. 48 (1977) 702–710.
[15] A. Payne, Shielding of magnetic fields by eddy currents, on the world-wide web at g3rbj.co.uk/.